Received: 10 June 2020 | Accepted: 27 August 2020

DOI: 10.1002/app.50098

ARTICLE

Applied Polymer SCIENCE WILEY

Wettability alteration of oil-wet carbonate rocks by chitosan derivatives for application in enhanced oil recovery

Agatha Densy dos Santos Francisco | Daniel Grasseschi | Regina Sandra Veiga Nascimento

Chemistry Institute, Federal University of Rio de Janeiro (UFRJ), Rio de Janeiro, Brazil

Correspondence
Regina Sandra Veiga Nascimento, Universidade Federal do Rio de Janeiro, Instituto de Química, Rua Hélio de Almeida 40, Rio de Janeiro, RJ 21 941614, Brazil.
Email: resinasandra@yahoo.com.br

Funding information
CNPq, CAPES, and Petrobras

Abstract

The increasing demand for oil and the fast decline of crude oil production from mature fields encourages the development of new enhanced oil recovery (EOR) technologies. In this work, trimethyl chitosan (TMC) and trimethyl chitosan hydrophobized with myristoyl chloride (TMC-C14) are synthesized, and their wettability modification capacity of oil-wet carbonate rocks is evaluated through contact angle measurements, atomic force microscopy, and Raman spectroscopy. Their interaction with asphaltene molecules was evaluated through UV–Vis spectroscopy. Transport behavior and oil displacement capacity were investigated in an unconsolidated porous medium. Results show that they can modify the wettability of oil-wet carbonate rocks, turning them water-wet, promoting oil displacement increases by 25% for TMC, and 16% for TMC-C14.TMC shows a better performance for wettability alteration than TMC-C14, confirming the hypothesis that the higher the positive charge density on the polymeric surfactant structure, the more efficient will be the system as a wettability modifier and as an EOR agent.

KEYWORDS

chitosan, EOR, oil and gas, polysaccharides, structure-property relationships, wettability

1 | INTRODUCTION

The energy consumption levels have been increasing in recent decades, and despite all the efforts to move to a cleaner energy matrix, the dependence on fossil fuels, such as oil, is still very strong. However, according to the annual report of OPEC[1] (Organization of the Petroleum Exporting Countries), the world oil demand growth in recent years was marginally revised in some countries. Apart from that, oil production has always been strongly influenced by oil prices, and at the beginning of 2020, there was a significant price reduction, mainly caused by the COVID-19 pandemic, which has been promoting an impact in the oil production around the world.[2,3] A fast decline of the crude oil production and the still great demand for it have been forcing the industry to develop new technologies for enhanced oil recovery (EOR) that would improve the production not only from matured fields, where up to 60% of the original oil in place (OOIP) is still unrecovered after the conventional primary and secondary recovery techniques have been employed but also from new fields.[4] The improvement of the oil production methods may contribute to decreasing the oil production costs, and in this scenario, EOR can play an essential role in achieving a substantial profit raise.[5] These events become even more critical and necessary for the development of new technologies for EOR that would be efficient, sustainable, and of low cost, as proposed in this work.

The main methods employed in EOR can be classified as thermal, microbiological, miscible, and chemical processes.[2] The oil retention that occurs in the reservoir pores is mainly due to factors such as strong capillary forces in the rocks pores, oil-wet rocks surface wettability, low viscosity of injected fluids, and specific intermolecular interactions at the rock–oil–water interfaces. EOR chemical methods are usually based on the reduction of the oil/water interfacial tension, the improvement of the injected fluid sweeping efficiency, and the rock wettability modification (WM) to allow for an enhancement of the oil displacement in the reservoir. Surfactants or alkalis can reduce the capillary forces by increasing the capillary number (CN) through a decrease of the interfacial tension. Polymers, on the other hand, increase the injected fluid viscosity improving the sweeping efficiency of the system[3]. Increasing CN is known to enhance oil production, and the contact angle between the injected fluid and rocks surface is one of the parameters used to monitor CN changes, and consequently, the rocks wettability.[4] Generally, it is more difficult to displace hydrocarbons from oil-wet reservoirs. Therefore, it is crucial to modify the wettability of reservoir rocks, turning them water-wet, and improving the flow behavior of the system.

The wettability of oil reservoirs has been intensively studied, and asphaltenes (the components of the most aromatic and polar hydrocarbons fraction in the crude oil) are considered to be the main responsible for turning carbonate rocks oil-wet.[5] Recently, cationic surfactants and metallic oxide nanoparticles have been used in WM processes, and cationic surfactants, such as the commercial cetyltrimethylammonium bromide (CTAB), are recognized as some of the most efficient, where the contact angle, Fourier transformed infra-red (FTIR), atomic force microscopy (AFM), and zeta potential techniques are frequently employed in the evaluation of their efficiency.[6–8] Hou et al. determined the WM mechanisms promoted by different surfactants through AFM, zeta potential, and contact angle measurements. They showed that ion-pair formation, adsorption of the surfactant on the solid surface by hydrogen bonds, and hydrophobic interactions and also electrostatic repulsion between the negatively charged head groups were the primary mechanisms for cationic, nonionic and anionic surfactants, respectively.[6,7]

The literature is continually reporting on the importance of the charge density on the surfactant head for the modification of the wettability of oil-wet rocks. Salehi et al. demonstrated the efficiency of a biosurfactant named surfactin, which presented a high-charge density on the headgroup, and proposed that the wettability alteration processes might be improved through the use of dimeric surfactants.[9] Later, Hou et al. have also shown that there were fewer asphaltene particles left on a solid surface treated with a cationic gemini surfactant and that they had the most robust ability to change the surface wettability when compared with other surfactants, and because of that, it produced the highest oil recovery.[7] Zhang et al. have studied the wettability alteration promoted by a trimeric cationic surfactant at mica mineral surfaces, and compared that with the modification promoted by single- and double-chain cationic surfactants, concluding that the trimeric was a more effective wetting agent.[8] Karimi et al. observed, by FTIR modifications of calcite surfaces before and after being oil-treated and surfactant-treated in the presence of salt.[10,11] Nicolini et al. has studied low-salinity systems, and they have confirmed that the rock wettability could be improved in low-salinity water toward a more water-wet condition, therefore improving oil recovery.[12]

The most accepted WM mechanism by cationic surfactants is the formation of ionic pairs between their positively charged polar head and the negatively charged groups present in the asphaltenes structures, mainly carboxylates.[13] Zhang et al. showed that the higher the surfactant charge density, the greater its potential to modify the rocks' wettability.[8] In addition, for some materials such as the metallic oxide nanoparticles, their high-adsorption capacity and affinity for asphaltenes[14,15] could probably explain their good performance as WM agents. However, no study has been reported to establish a relationship between their affinity for asphaltenes and WM capacity.

Despite their high efficiency, the use of some ionic surfactants in EOR processes should be carefully evaluated due to their high production cost, high toxicity, and tendency to adsorb on the reservoir rocks surface. Usually, to minimize losses by adsorption, anionic surfactants are employed in sandstone reservoirs, while cationic surfactants are used in carbonate reservoirs.[16] The use of macromolecules or nanomaterials as surfactant carriers has also been evaluated as an alternative to reduce surfactants adsorption on the rocks surfaces.[17–21]

In this scenario, the development of alternative materials that would combine the advantages of surfactants and polymers would be extremely important for the oil industry. Polymeric surfactants represent an attractive alternative since they can simultaneously provide an increase of the water viscosity, a decrease of the interfacial tension, and a WM, all very beneficial to the EOR process efficiency.[22,23] Chitosan derivatives could act as polymeric surfactants combining both effects of modifying the rock wettability and improving the sweeping efficiency in EOR applications. The use of chitosan derivatives as WM agents has not been yet explored in

TABLE 1 Carbonate rock grains mineral composition

Composition
$CaCO_3$
CaO
SiO_2
MgO
Al_2O_3

the literature and shows interesting perspectives, since these materials are water-soluble, produced from an abundant fishing industry waste, and present low toxicity when compared with commonly used cationic surfactants, such as CTAB, that presents a localized single positive charge. On the other side, the unmodified chitosan dissolves exclusively in acidic medium, which would not meet the normal EOR operational conditions, especially in carbonate reservoirs, where the wettability problems are usually more severe.

The present study evaluated the potential of the water-soluble cationic chitosan derivatives trimethyl chitosan (TMC) and trimethyl chitosan hydrophobized with myristoyl chloride (TMC-C14) as wettability modifiers of oil-wet carbonate rocks in EOR processes. The chitosan derivatives TMC and TMC-C14 were synthesized through quaternization and hydrophobization reactions, respectively,[24–26] and their capacity to act in the WM of oil-wet calcite crystal fragments was studied by the contact angle, AFM, and Raman spectroscopy. The distribution of positive charges along the polymeric structure provided water solubility to the polysaccharide structure and lead to a greater affinity for asphaltenes, as compared to the contact angle results for CTAB, which presents a localized single positive charge. Consequently, the chitosan derivatives (TMC and TMC-C14) were able to modify the wettability of oil-wet carbonate rocks better, turning them wet by water or brine solutions and leading to lower contact angles. Raman spectroscopy provided valuable information on the interaction between the rock surface and the oil components, allowing the evaluation of the WM agent effect on the rock surface due to interactions with specific fractions of asphaltenes. The use of Raman spectroscopy in the investigation of WM processes for EOR is scarce and could be more explored as a simple, fast, and quantitative low-cost technique. In addition, transport behavior and oil displacement experiments in unconsolidated carbonate porous medium showed that TMC and TMC-C14 were able to permeate through the porous medium with very low-retention rate, which has helped to promote an increase of 25% in the residual oil production, reaching a total oil recovery factor of 51%.

2 | MATERIALS AND EXPERIMENTAL METHODS

2.1 | Materials

2.1.1 | Materials used for the synthesis of chitosan derivatives

The commercial chitosan (CHI) of low-average molecular weight and deacetylation degree of 75–85%, myristoyl chloride, 1-methyl pyrrolidone, methyl iodide, sodium iodide, sodium hydroxide, acetic acid, hydrochloric acid, hexadecyltrimethylammonium bromide (CTAB), and methanol were purchased from Sigma-Aldrich Corporation and used as received.

2.1.2 | Crude oil

The crude oil with API° of 38 and 0.86 wt% of asphaltene content used in this research was obtained from one of the Brazilian oil reservoirs and kindly supplied by Petrobras.

2.1.3 | Seawater (brine)

Synthetic brine with 3 wt% NaCl + 0.1 wt% $CaCl_2$ + 0.1 wt% $MgCl_2$ concentration was prepared using chemicals purchased from Vetec Química Fina Ltda without previous treatment.

2.1.4 | Carbonate rocks: Calcite fragments and carbonate rock grains

For contact angle measurements, calcite fragments of 1 cm^2 were used. Carbonate rock grains with 40–70 mesh of particle size, purchased from Brasil Minas Indústria e Comércio Ltda and whose composition is shown in Table 1, were used for obtaining the unconsolidated porous medium.

2.2 | Experimental methods

2.2.1 | Chitosan derivatives synthesis

The chitosan derivatives were synthesized from the CHI. The products were named as TMC for the cationized derivative (trimethyl chitosan) and TMC-C14 for the cationized and partially hydrophobized derivative, where C14 refers to the number of carbon atoms of the inserted

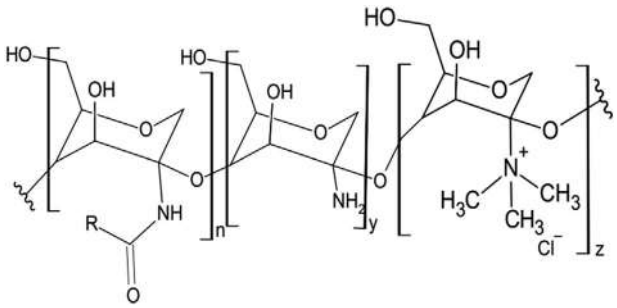

FIGURE 1 Chitosan derivatives structures (TMC → R = CH_3 while TMC-C14 → R = $CH_3[CH_2]_{12}$). TMC, trimethyl chitosan

(alkyl hydrophobic) segment, as shown in Figure 1. Trimethylated cationic chitosan (TMC) was obtained by a quaternization reaction using CH_3I, following an adaptation from the procedure described by Domard et al.[24] and described in our previous work.[25] The hydrophobic and cationic chitosan (TMC-C14) was obtained by a two-step procedure with the combination of hydrophobization with myristoyl chloride from Le[27] and Domard quaternization reactions. The obtained TMC is soluble in water over a broad range of pH, while the obtained TMC-C14 is partially soluble in water, in contrast to chitosan, which is only soluble in pH < 6. The final products were characterized by FTIR, and the trimethylation or cationization degrees (CD) were determined by solid-state ^{13}C NMR (see Lopes et al. to more informations).[25]

2.2.2 | Asphaltenes extraction

To evaluate the affinity between asphaltenes and the chitosan derivatives, the asphaltenes were precipitated from the carbonate reservoir crude oil following the procedure described by Franco et al.[28] An excess of n-heptane was added to the crude oil at a 40/1 ratio. The mixture was sonicated (Hielsher, model UP205) for 2 h at 25°C and thereafter placed in a thermostatic stirring bath (Nova technique NT230) at 220 rpm for 24 h. After this period, the asphaltene samples were centrifuged at 3300 rpm for 30 min. The extracted solid was washed with n-heptane several times until it showed a brilliant black color. The sample was then dried at room temperature, and the solid obtained was ground with grail and pistil, and dissolved in toluene to obtain an asphaltene stock solution at a concentration of 2000 mg/L. The obtained asphaltene solution was subjected to UV–Visible spectroscopy using a Shimadzu UV2450 spectrophotometer. An analytical curve was built, and the absorbance at 283 nm was chosen to quantify the asphaltene in solution.

2.2.3 | Evaluation of the interaction between asphaltenes and the chitosan derivatives

To evaluate the interaction between asphaltenes and the chitosan derivatives, their solutions were mixed at 25°C for 24 h, and after this, the content of asphaltene remaining in solution was quantified. The systems were prepared by adding 10 ml of an asphaltene solution in toluene at different concentrations (80–2000 ppm) to flasks containing 10 ml of a TMC or TMC-C14 solution at 5000 ppm. The systems were sonicated for 3 min to form an emulsion, increasing the contact area. After the emulsion was formed, it was stirred at 200 rpm for 24 h. Next, the systems were centrifuged at 3300 rpm for 30 min, and the supernatant (containing the asphaltene solution) was collected for analysis with the UV–Vis spectrophotometer.

2.2.4 | Aging process of the calcite crystals surface

New calcite crystals, used to model reservoirs carbonate rocks, were cleaved to obtain fragments in the form of small platelets with face areas of approximately 1 cm^2. The fragments were aged (turned oil-wet) by immersion in crude oil, being kept at 70°C for at least 72 h. The calcite crystal fragments were then washed with heptane and oven-dried at 70°C. The results of this aging process were evaluated by contact angle measurements on both crystal faces at the air–water–rock interface, and just the calcite fragments that presented contact angles of water droplets ≥90° were used to evaluate the WM that would have been promoted by the treatment step with the chitosan derivatives.

2.2.5 | Evaluation of the wettability modifier performance by contact angle measurements

A series of solutions/suspensions of the WM agent (TMC or TMC-C14) at different concentrations (100–5000 ppm) was prepared by dissolving the agent in water or brine. An oil-wet calcite fragment, with a known contact angle (≥90°), was immersed in the chitosan derivative solution/suspension and kept in a shaker for 24 h at room temperature. After that period, the calcite fragment was washed with water and dried at 70°C for 24 h. The contact angle between a droplet of water, calcite fragment surface, and air was measured with a Phoenix Mini SEO

goniometer. Taking the contact angle value of the aged calcite fragment before and after the WM treatment, the reduction percentage of the contact angle value was calculated.

2.2.6 | AFM images

AFM images were collected using a Flex AFM (Nanosurf) microscope with C3000 controller (Nanosurf) operating in the contact AFM mode, recording 256 pixels images with a scan speed around 0.40 Hz, and contact AFM tip from the Budget Sensors model Multi-75Al-G.

2.2.7 | Raman spectroscopy

Raman spectroscopy was performed using a micro-Raman spectrometer (NT-MDT, NTEGRA SPECTRA) equipped with a CCD detector and solid-state laser at an excitation wavelength of 473 nm. All the measurements were performed using a 100X magnification objective producing a laser spot of the order of 1 μm with an incident laser power of less than 0.20 mW, 50 s integration time, and single accumulations.

2.2.8 | Transport behavior evaluation of the chitosan derivatives through a carbonate unconsolidated porous medium

Dynamic test unit

The dynamic tests were performed in an injection system consisting of a chromatography column (2.5 cm of diameter, 15 cm of length), sealed at both ends by screw caps with 20 μm filters, and 1/8″ outside diameter hoses, as depicted in Figure 2. A MasterFlex L/S Cole-Parmer peristaltic pump was used to inject the fluids. The column was filled with carbonate rocks with grain sizes between 40 and 70 mesh. It provided an unconsolidated porous medium with 25% porosity, measured by real grain density and a pore volume (PV) of 30 ml. The system was sealed and all fluids were injected at a 1 ml/min flow rate. The transport tests consisted of saturating the system with water or brine, followed by the injection of two PV of the WM agent (TMC or TMC-C14) solution and ending with an injection of three PV of water or brine. The effluent was collected at $\frac{1}{3}$ PV intervals and analyzed by TOC (Total Organic Carbon Analyzer, TOC-L Shimadzu). The relative WM agent concentration (C/C_0) was plotted as a function of the number of injected PV to generate the breakthrough curves, that is, the relative concentration versus PV. The objective of this test was available the content of chitosan derivatives retained in medium porous after polymer flooding.

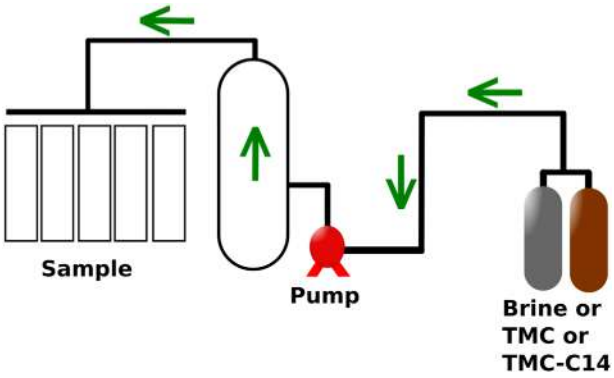

FIGURE 2 Unconsolidated porous medium unit scheme. TMC, trimethyl chitosan [Color figure can be viewed at wileyonlinelibrary.com]

2.2.9 | Oil recovery test in the unconsolidated porous medium

The dynamic test unit (Figure 2) was also used for the oil recovery test. The dynamic test unit was tested several times with water or brine to evaluate the reproducibility of the flooding experiment. The main parameters as porosity, grain size, and injection flow were adjusted to obtain the best performance.

For this purpose, the carbonate powder (0.420–0.210 mm) was aged in oil (75% crude oil + 25% heptane) for 48 h at 70°C, before being introduced in the column to form the unconsolidated porous medium. To evaluate the efficiency of TMC and TMC-C14 in the oil displacement, the system was sealed, and the pump was preprogrammed for a 0.5 ml/min injection flow. The first part of the test consisted of the secondary recovery phase simulation, where four PV of brine were injected. After this step, the EOR phase was initiated, and one PV of a chitosan derivative solution (TMC or TMC-C14–0.50 wt%) in brine was injected, and the system was allowed to rest for 24 h. After this time, another five PVs of brine were injected into the porous medium. The effluent was collected at $\frac{1}{3}$ PV intervals in 10 ml graduated cylinders, and the oil content was analyzed by volume measurements. The OOIP was calculated.

3 | RESULTS AND DISCUSSION

3.1 | Synthesis and characterization of chitosan derivatives

The chitosan derivatives were successfully synthesized. FTIR and solid-state ^{13}C NMR characterization

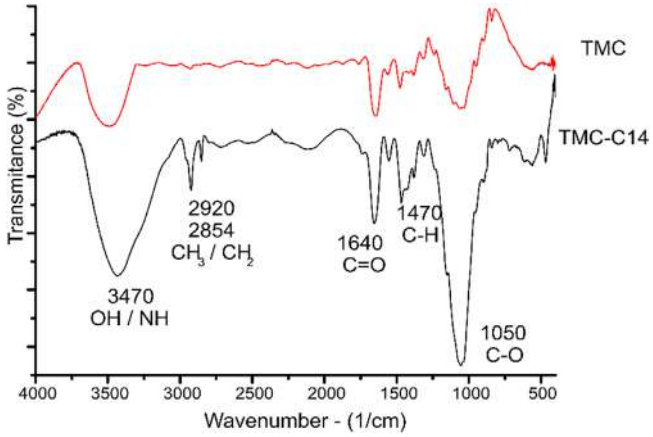

FIGURE 3 Infrared spectra of TMC and TMC-C14. TMC, trimethyl chitosan [Color figure can be viewed at wileyonlinelibrary.com]

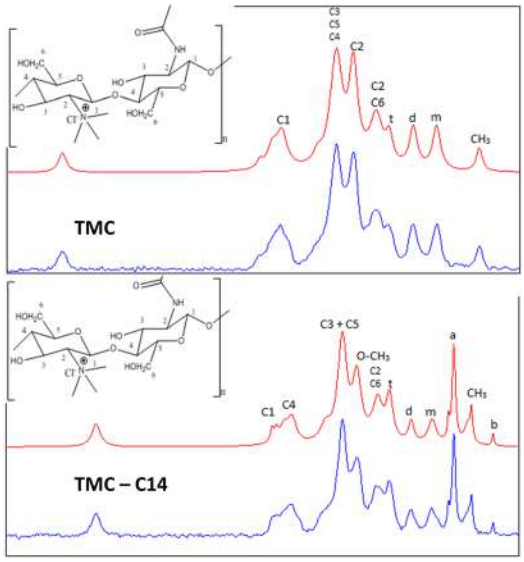

FIGURE 4 ^{13}C NMR spectra of TMC and TMC-C14. TMC, trimethyl chitosan [Color figure can be viewed at wileyonlinelibrary.com]

confirmed that the chemical modifications were performed (Figures 3 and 4 and Table 2). The obtained products were very similar to the ones from the previous work of our group. The cationic degree (CD), extracted from ^{13}C NMR was 23% for TMC and 8% for TMC-C14 whose structures are shown in Figure 1. The CD was calculated using equations from Lopes[25] by deconvolution of ^{13}C-NMR spectra in the program Dmfit (red line in NMR spectrum). The CD and the distribution of the charges along the polymeric structure are important parameters for the rock WM capacity of the agent, and it will be discussed later.

3.2 | Evaluation of the interaction between asphaltenes and chitosan derivatives

The interaction of asphaltene with specific EOR agents, such as metal oxide nanoparticles, has been discussed in the literature.[28–32] However, no reports were found on the interaction of asphaltenes with macromolecules in solution, although chitosan has been used to encapsulate organic molecules.[33–36] TMC and TMC-C14 chitosan derivatives should be able to interact with asphaltenes from carbonate reservoirs oils through ionic pairs formation between the carboxylate groups present in the asphaltene molecules and the quaternary ammonium cationic groups from the derivatives forming a complex, or in the case of the TMC-C14 derivative, through hydrophobic interactions of its hydrocarbon chains with the linear chains commonly found in asphaltenes structures.[37–39]

To evaluate the affinity between asphaltene molecules and the chitosan derivatives, their solutions in toluene were mixed at several concentrations, and the initial asphaltene concentration in the toluene solutions ranged from 50 to 2000 mg/L, covering conditions of asphaltene nanoaggregation and cluster formation.[40,41] After 24 h of contact, the chitosan derivatives were precipitated by centrifugation, and the asphaltene content in solution at the equilibrium was obtained by UV–Vis Spectroscopy. Figure 5 shows the asphaltene content that interacted with TMC and TMC-C14.

For the studied concentrations, TMC has shown an asphaltene saturation three times higher than the one shown by TMC-C14 (Figure 5). TMC is a cationic polymer whose positive charge is scattered throughout its molecular structure, and the sample employed in this study has a CD of 23%, while TMC-C14 is an amphiphilic polymer with a CD of 8%. One could suggest that the higher the number of positive sites (active sites) higher would be the affinity and interaction of the chitosan derivative toward the asphaltene. However, the hydrophobic groups may also contribute and have an influence on the performance of the polysaccharide. These results indicate that both chitosan derivatives should be able to interact favorably with asphaltenes and therefore, modify the rock wettability.

3.3 | WM study

3.3.1 | Contact angle

The contact angle measurement is the most widely accepted method for evaluating reservoir wettability.[4] For cationic surfactants, the suggested WM mechanism is based on their adsorption on the rock's surface, followed

TABLE 2 Chemical shifts from solid-state ^{13}C-NMR spectra of chitosan derivatives

TMC peaks	Chemical shift (ppm)	TMC-C14 peaks	Chemical shift (ppm)
C1	102.2–95.2	C1	102.2–95.2
C3 + C5 + C4	74.8	C3 + C5 + C4	74.8
C2	68.4	C2	68.4
C2 + C6	60.6	C2 + C6	60.6
t	55.6	t	55.6
d	46.6	d	46.6
m	38.8	m	38.8
CH_3	23.2	a	29.8
–	–	CH_3	23.2

Abbreviation: TMC, trimethyl chitosan.

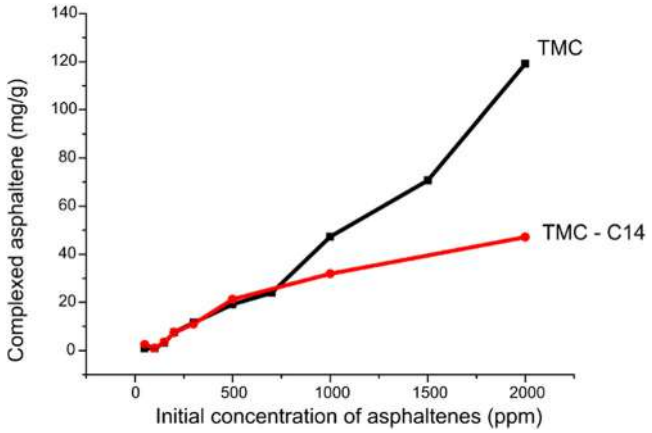

FIGURE 5 Saturation curves of asphaltenes with TMC or TMC-C14 macromolecules at the equilibrium. TMC, trimethyl chitosan [Color figure can be viewed at wileyonlinelibrary.com]

by the asphaltene desorption caused by the interaction between the surfactant cationic polar head and the carboxylate groups present in the asphaltene molecules, forming an ion-pair.[6,13] The ionic pair could desorb from the rock surface and become stabilized inside surfactant micelles previously formed in the aqueous medium. The chitosan derivatives showed a great affinity for asphaltenes, as shown by the curves in Figure 6. They were evaluated as WM agents of calcite fragments by contact angle measurements at the surface–water–air interface, and their performance was compared to that of CTAB. Figure 6 shows the contact angle reduction obtained with TMC and TMC-C14 solutions on oil-wet calcite fragments aged in crude oil (see the experimental section). The results show that both the chitosan derivatives (TMC and TMC-C14) were able to modify the wettability of oil-wet calcite fragments, presenting a great decrease of the contact angle from concentrations of 1000 ppm. In other words, the chitosan derivatives turned the crystals water-wet, as did the commercial surfactant CTAB. The contact angle of water droplets after the WM agents treatment at a concentration of 5000 ppm was of 30° for TMC, 45° for CTAB, and 60° for TMC-C14. With brine, the following contact angles were observed: TMC (30°), TMC-C14 (45°), and CTAB (70°). The wettability depends strongly on the pH, salinity conditions, and also on the nature of the oil and the rock.[42] The presence of salts did not change the TMC performance for contact angle reduction (70%); however, there was a significant improvement for the TMC-C14 (40 → 60%) efficiency and a decrease in the CTAB performance (50% → 30%), as also reported by Kumar et al.[43] The presence of brine decreased the solubility of TMC-C14. Consequently, at the equilibrium, its adsorption was displaced toward the calcite surface covered by adsorbed asphaltene molecules, improving its efficiency as a WM agent. The order of efficiency for the WM was TMC > CTAB > TMC-C14 in water and TMC > TMC-C14 > CTAB in brine. Most of the currently explored wells in Brazil are in the presalt region and feature extremely high salinities. Therefore, the nontoxic chitosan derivatives could be used as WM agents in those fields, even in highly saline media.

To understand the difference in performance between the chitosan derivatives and the commercial surfactant, it is necessary to consider the number of cationic sites of each additive. TMC is a polymer whose cationic groups are scattered throughout its macromolecular structure, with a great number of active sites available to interact with the carboxylate groups present in the asphaltene structure. On the other hand, CTAB is a small molecule with a single positive charge located on the surfactant polar head. Therefore, chitosan derivatives were more efficient than CTAB in reducing the contact angle. These derivatives were able to interact with a higher number of active sites of the asphaltenes structure.

The TMC-C14 have shown a different performance from the one presented by TMC, not only because of its

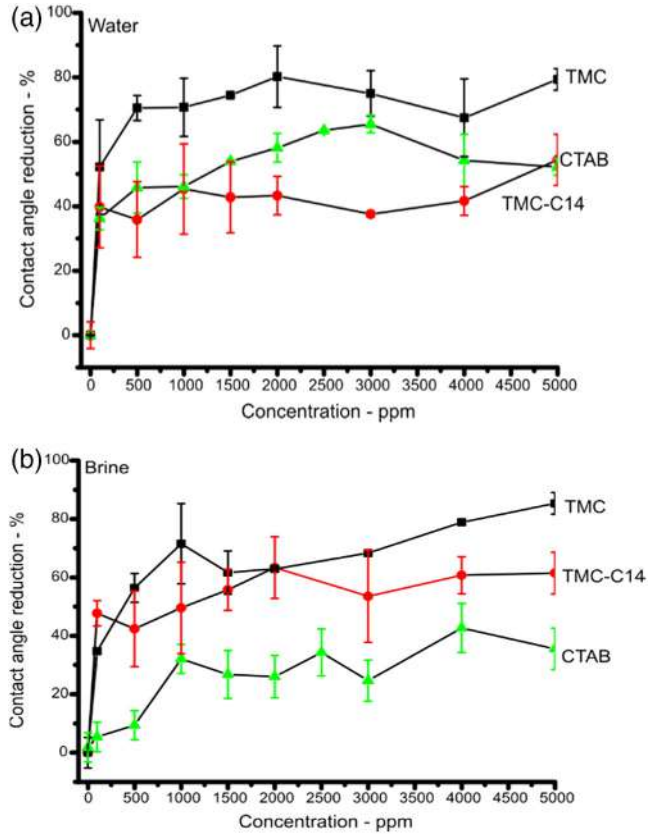

FIGURE 6 Effect of TMC, TMC-C14, and CTAB solutions concentration on oil-wet calcite surfaces contact angle reduction (a) in water, (b) in brine. CTAB, cetyltrimethylammonium bromide; TMC, trimethyl chitosan [Color figure can be viewed at wileyonlinelibrary.com]

lower number of cationic groups along with its molecular structure but due to a different WM mechanism that could contribute to its effectiveness as WM agent. In this second mechanism, the hydrophobic segments present in its molecular structure would be reorganized, with their hydrophobic tails interacting with the adsorbed asphaltenes and forming a thin film on the rocks surface, as suggested by Zhang et al. and other authors.[6,8,23]

The contact angle results showed that TMC is more efficient than TMC-C14, and to elucidate the possible mechanisms of action for each derivative, AFM and Raman analysis of the calcite surfaces were performed before and after the treatment with the two chitosan derivatives.

Atomic force microscopy

AFM is a convenient technique for showing the changes in sample surfaces. It is commonly used to help reflect wettability alteration mechanisms.[44] Al Nassari et al. studied by AFM the effect of irreversibly adsorbed nanoparticles on the surface roughness.[4,45] While Xie et al. used AFM together with other techniques to understand the importance of basal-charged clays during low-salinity water flooding in sandstone reservoirs.[46] Shaik et al. studied the effect of brine and ionic strength on the wettability alteration of naphthenic-acid-adsorbed calcite surfaces by AFM.[47] Similar with this work, Hou et al. utilized AFM to make clear the mechanism for wettability alteration of oil-wet sandstone surface using different surfactants.[6] The surface roughness and the height profile of the calcite fragments were evaluated by AFM, before and after the WM treatment, in a tentative to correlate with the WM results[4,6,8,29,38,42,45,48] and to understand how the chitosan derivatives would be acting in the process.

Figures 7(a) through 7(d) show the AFM images of different samples and their respective height profile. Figure 7(a) refers to the fresh calcite, Figure 7(b) to the oil-aged calcite, and Figure 7(c), and also Figure 7(d) are related to calcite fragments that have been aged and subjected to treatment with TMC and TMC-C14, respectively. As expected, the fresh calcite has shown a homogeneous surface whose height profile and roughness values (Sq = 0.929 nm) indicated the absence of adsorbed material on its surface. On the other hand, the oil-aged calcite presented a heterogeneous surface, with a squared roughness value of 26.59 nm and sharp variations in the height profile, as shown in Figure 7(b),(f). This surface roughness value (Table 3) is a strong indication of the presence of an adsorbed layer on the fragment surface.[49] The oil-aged calcite fragments treated with the chitosan derivatives did show an evident topography change of their surface. The calcite fragment treated with TMC presented a homogeneous surface with a roughness around 1.13 nm, with some 10 nm height features distributed on the surface (Figure 7(c)). The analysis of these data shows that the surface treated with TMC showed a high degree of similarity with the one for the fresh calcite, suggesting that the initially adsorbed asphaltenes were removed from the rock's surface, as already indicated by the contact angle tests results. Hou et al. also observed the absence of the asphaltenes layer from the rock's surface after the treatment with CTAB of an oil aged mica fragment.[6] The main reason for the roughness reduction was attributed to the desorption phenomenon from the solid surface by ionic pairs formed in the process.[6] On the other hand, the TMC-C14 treatment resulted in a heterogeneous surface, although with a different topography from the oil-aged fragment. The decrease of the roughness value (Sq = 18.21 nm) suggests that a fraction of the asphaltene might have been removed from the rocks surface and the topographic changes (Figure 7(d)) suggest the formation of a TCM-C14 film on the top of the remaining asphaltene molecules still adsorbed on the calcite surface. Zhang et al. showed that the increase of alkyl groups in the surfactant

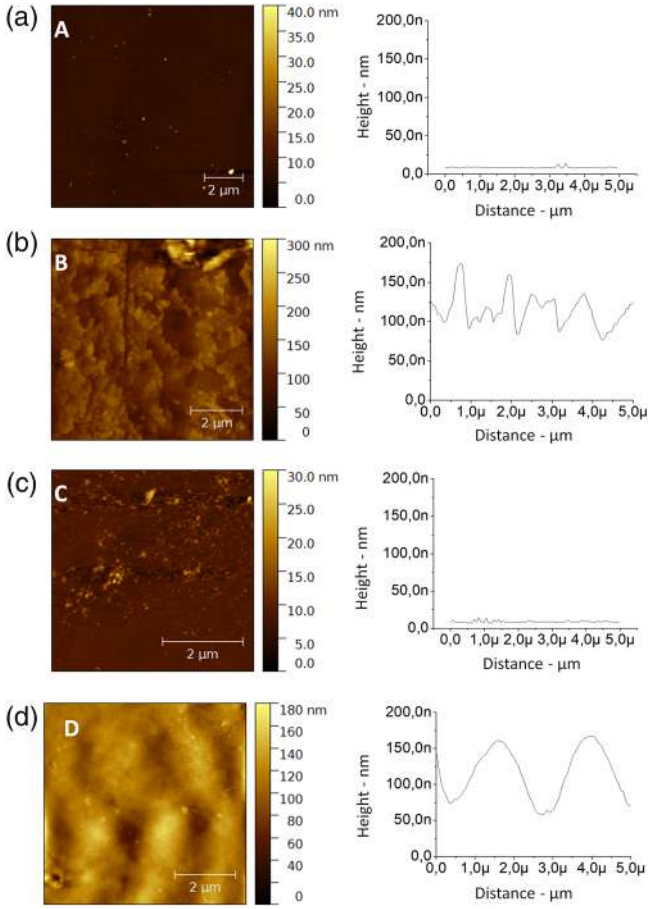

FIGURE 7 AFM images of different samples (a) fresh calcite, (b) aged calcite, (c) aged calcite treated with TMC, (d) aged calcite treated with TMC-C14. AFM, atomic force microscopy; TMC, trimethyl chitosan [Color figure can be viewed at wileyonlinelibrary.com]

TABLE 3 Calcite surface roughness

Calcite	Sq[a] (nm)	Sa[a] (nm)
Fresh	0.929	0.4444
Oil-wet	26.59	19.84
Oil-wet treated with TMC	1.13	0.764
Oil-wet treated with TMC-C14	18.21	14.33

Abbreviation: TMC, trimethyl chitosan.
[a]Sq and Sa is a roughness.

structure, as well as the increase of their concentration, also causes a change in the height profile of the layer formed on the surface of mica.[8]

3.3.2 | Raman spectroscopy

Due to Raman spectroscopy's high sensitivity to carbon materials, especially polycyclic aromatic hydrocarbons, the technique was used to observe possible changes in

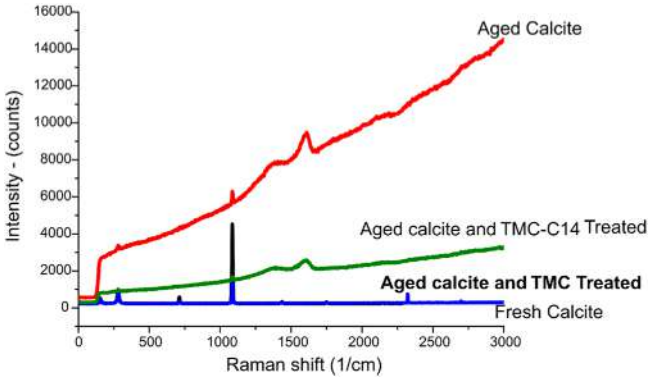

FIGURE 8 Raman spectra of different samples: Fresh calcite (black curve), aged calcite (red curve), aged calcite treated with TMC (blue curve), and aged calcite treated with TMC-C14 (green curve). TMC, trimethyl chitosan [Color figure can be viewed at wileyonlinelibrary.com]

the surfaces caused by the asphaltenes adsorption/desorption processes. Raman spectra were collected from the surface of fresh, oil-aged, and also from TMC or TMC-C14 treated calcite fragments. Figure 8 shows the Raman spectrum (black curve) of a fresh calcite surface, which presents the characteristic bands of $CaCO_3$. The typical bands of calcite, which is the most stable polymorph of $CaCO_3$, was observed at 155 cm^{-1} (C-O-translation), 277 cm^{-1} (C-O-torsion), 683 cm^{-1} (C-O-C-in-plane deformation), 1063 cm^{-1} (C-O s-stretching), and 1411 cm^{-1} (C-O a-stretching).[50]

As expected, in the oil-aged calcite spectrum (red curve in Figure 6) the D and G bands can be observed at 1370 and 1600 cm^{-1}, respectively, and attributed to asphaltenes adsorbed on the calcite surface. Besides, there is an increase in the baseline due to the asphaltene fluorescence. G and D are the typical bands of organized carbon materials such as asphaltenes and graphite. The G band corresponds to the stretching vibration of sp^2-like carbon atoms within the aromatic hexagonal sheet as well as those sp^2-like atoms in lateral chains. The D band corresponds to the C–C forbidden stretching modes that become active due to defects in the aromatic structure. In the case of asphaltenes the boundaries of the ordered aromatic structure, the presence of five-membered rings and heteroatoms are the primary defects responsible for the observation of the D band in the Raman spectra.[51–53]

The oil-aged calcite fragment treated with TMC restored the fresh calcite bands, indicating complete removal of asphaltene by TMC (blue curve in Figure 8). However, in the spectra for the calcite fragment treated with TMC-C14 is difficult to observe the typical $CaCO_3$ bands due to the asphaltene layers that remained on the surface, which were confirmed by the presence of the D and G modes (green curve in Figure 8). However, their

intensity reduction suggests that some asphaltene layers were desorbed. Thus, Raman spectroscopy confirms that the chitosan derivative TMC is capable of removing most of the asphaltene layers adsorbed on the calcite surface, as indicated by the contact angle measurements and microscopy images. In contrast, the TMC-C14 derivative removes only a few asphaltene surface layers, and the observed WM is mainly due to its adsorption on the calcite surface.

3.4 | Dynamic transport behavior of chitosan derivatives through the unconsolidated porous medium

The breakthrough curves are obtained through of dynamic transport test. It shows a capacity of chitosan derivatives in permeate through an unconsolidated porous medium and that it is done to check if the material to be injected will be able to reach the region of the reservoir where the crude oil is located, it is the main objective of this test.

The adsorption of the injected chemical agents on the reservoirs rock's surface can significantly affect the chemical EOR flooding processes negatively, both from the technical and economic perspectives, decreasing the oil recovery efficiency and delaying the occurrence of the chemical and oil breakthroughs.[54] The surface chemistry of carbonates in aqueous solutions has an important influence on the process of surfactant adsorption. Commonly, it is supposed that the surface of the carbonate rocks is positively charged.[55] In order to minimize adsorption losses, cationic surfactants are preferably used in carbonate formations to take advantage of the repulsive electrostatic interactions.[16]

The dynamic transport results showed that, in water, the chitosan derivatives behaved similarly to the commercial cationic surfactants, being able to permeate through an unconsolidated porous medium, with no significant adsorption on the carbonate rocks, as shown in the breakthrough curves of Figure 9.[56–58] In this case, it is believed that the electrostatic repulsion that occurs between the $N^+(CH_3)_3$ positive charges on the polymers (TMC and TMC-C14) and the ones on the carbonate surface is the responsible for the low adsorption. This behavior is desirable for EOR applications since the costs caused by adsorption losses can make the operation unfeasible.

The chitosan derivatives, when dissolved in brine, did not permeate very well through the porous medium composed of carbonate rocks, as shown in the breakthrough curve in Figure 9. About 15% of the injected material was retained within the porous medium, that is, the TMC and TMC-C14 macromolecules were either adsorbed on the carbonate rocks or were not able to pass through the pores, an event that was not observed in the experiment with pure water. Since chitosan derivatives are polymers, the presence of salt may have reduced their solubility, which could lead to the formation of aggregates and hinder their displacement through the porous medium. Apart from that, some studies point out that although surfactants or cationic polymers do not have a natural tendency to adsorb on carbonate, this phenomenon may occur due to the presence of contaminants such as silica and clay, which have a negative surface charge.[56] In this case, the negative surface of the clay minerals present in the carbonate rock, as indicated by the results shown in Table 1, could interact with the $N^+(CH_3)_3$ groups present in the polymeric structure of the chitosan derivatives.

The cost of the gram of an EOR additive adsorbed per gram of rock ($g_{additive}/g_{rock}$) is an important parameter for the petroleum industry because it is related to the process costs. In this work, chitosan derivatives in the presence of brine showed an adsorption of 0.481 $mg_{(TMC)}/g_{(carbonate)}$ and 0.344 $mg_{(TMC\text{-}C14)}/g_{(carbonate)}$. The cationization degree (CD_{TMC} = 23%, $CD_{TMC\text{-}C14}$ = 8%) helps to understand the difference in adsorption between the two types of chitosan derivatives. Since the carbonate rocks used presented some fraction of clays, a greater amount of positive charge on the additive structure would lead to higher interaction between the polymer and the rock and consequently to greater adsorption.

The study by Saha et al. demonstrated the adsorption of Triton X-100 (nonionic surfactant) on Assam rock surface of 6.23 mg/g at a reservoir temperature of 70°C and using the reservoir formation water as the aqueous medium.[57] Also, literature values for surfactant adsorption onto a Berea core material range from 0.1 to 1.2 mg/g rock. Iglauer et al. shows that the adsorption of APG (Alkylpolyglycosides) surfactants on a solid surface is dependent on the APG alkyl chain length and that a larger chain length led to higher adsorption, reaching a value of 40 mg/g.[58] Comparing the adsorption values for the chitosan derivatives with some from the literature, it is apparent that they are considerably lower, which increases their potential for application in EOR.[57,58]

3.5 | Oil recovery test in an unconsolidated porous medium

The obtained results of WM and the affinity between asphaltenes and the chitosan derivatives, together with their low adsorption on the porous medium, suggest that the chitosan derivatives should be able to increase oil production during an EOR process. Thus, the chitosan

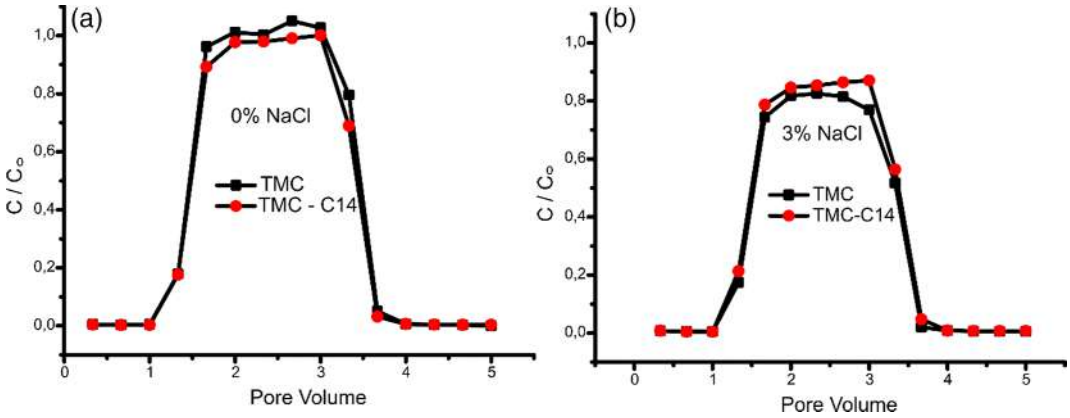

FIGURE 9 Breakthrough curves for TMC and TMC-C14 solutions-effluent concentration of TMC and TMC-C14 versus pore volume for the unconsolidated carbonate porous medium flood. Two PV of additives (0.50%) in 0% wt. NaCl (a) or 3% wt brine (b) were injected at 25°C and 1 ml/min. PV, pore volume; TMC, trimethyl chitosan [Color figure can be viewed at wileyonlinelibrary.com]

derivatives were evaluated for their ability to displace oil through unconsolidated carbonate porous medium experiments.

Figure 10 and Table 4 show the oil recovery factor obtained when the unconsolidated porous medium was flooded only with brine, simulating a secondary recovery and also when it was flooded with TMC or TMC-C14 brine solutions, thus simulating an EOR process. The results show that although the porous medium employed was an unconsolidated one, the secondary recovery was of about 25%, probably due to the aging stage, in agreement with the literature when the oil recovery is performed only with brine or water injections. The flooding tests in an unconsolidated porous medium often show higher recovery factors than those from core flooding, since the pore size and permeability in the unconsolidated medium are significantly higher. In addition, temperature, pressure, and the aging time of the reservoir's rocks with crude oil also have a significant influence on the EOR additive performance.[59–61] Although the literature shows that low-salinity systems are capable of decreasing the residual oil content, the flooding with just brine in the solution presented a poor performance, demonstrating the need for the implementation of an EOR process.[44]

The chitosan derivatives were able to satisfactorily increase the residual oil recovery factor in the porous medium experiment. TMC increased production by about 25% while TMC-C14 produced a displacement of about 16% higher. These results showed that chitosan derivatives have the potential to become suitable additives for EOR and their performance was much better than the ones from commercial surfactants as CTAB, or from nanoparticles,[6,62] mainly due to their ability to better modify the wettability, turning the porous medium more water-wet and then better facilitating the oil

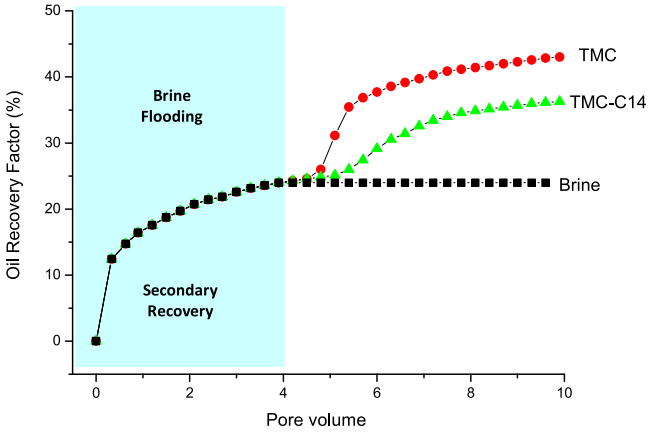

FIGURE 10 Oil recovery as a function of the injected pore volume. The enhanced oil recovery (EOR) began after the injection of four PV of brine with one PV of chitosan derivatives solutions (0.50 wt%) in brine at 25°C, and after this, five PV of brine were injected. The unconsolidated porous medium was previously aged for 48 h at 70°C. TMC, trimethyl chitosan [Color figure can be viewed at wileyonlinelibrary.com]

displacement.[63,64] The higher efficiency of TMC compared to the one of TMC-C14 may be related to the fact that besides presenting a higher interaction with asphaltenes, due to its higher number of cationic sites and also higher accessibility to those active sites for electrostatic interactions, this derivative (TMC) also promoted a more efficient contact angle reduction. On the other hand, the high affinity for asphaltene shown by TMC-C14, as confirmed by AFM results, could favor the adsorption of this derivative inside the porous medium due to hydrophobic interactions with the oil, thus making it more challenging to be used. The increased oil production promoted by the injection of chitosan derivatives should significantly increase the profits of the oil

TABLE 4 Summarized recovery results from flooding with brine and chitosan derivatives solution at ambient temperature

	Secondary oil recovery (%)	EOR (%)
Brine	25	–
TMC	26	25
TMC-C14	24	16

Abbreviations: EOR, enhanced oil recovery; TMC, trimethyl chitosan.

industry, however, further tests on consolidated porous media are needed to evaluate the chitosan derivatives behavior in a high temperature and pressure system.

4 | CONCLUSIONS

Generally, it is recognized that it is more difficult to displace hydrocarbons from oil-wet reservoirs than from the water-wet ones. The present work evaluated the potential of the cationic chitosan derivatives TMC and trimethylchitosan hydrophobized with myristoyl chloride (TMC-C14) as wettability modifiers of oil-wet carbonate rocks to be employed in EOR processes.

Contact angle measurements showed that the synthesized chitosan derivatives were able to modify the wettability of oil-wet calcite crystals in water and brine, allowing an increase of the residual oil recovery factor obtained in an unconsolidated carbonate porous medium. Thus, environmentally friendly chitosan derivatives emerge as promising EOR chemical agents that may replace toxic commercial cationic surfactants, such as CTAB.

Asphaltenes have been considered as the main responsible for turning carbonate rocks oil-wet, and their saturation curves obtained with the chitosan derivatives revealed that TMC has a higher capacity to interact with asphaltenes than TMC-C14. In this work, it was shown that there is a relationship between the wettability modifier capacity to interact with asphaltenes and its efficiency, where the higher is its interaction capacity, the better will be its performance as a WM agent. In addition, there is an influence of the number of cationic sites (CD) and their localization in the WM agent chemical structure on the WM capacity of the agent. The higher is the number of cationic sites of the molecule, the greater will be the agent potential as a wettability modifier of oil-wet rock surfaces and, therefore, its efficiency as EOR chemical agent.

Using AFM and Raman spectroscopy, it was proved that TMC is capable of removing most of the layers of asphaltenes adsorbed onto the calcite surface, while the TMC-C14 derivative became adsorbed on the residual asphaltenes layer. The presence of brine did not change the TMC performance to reduce the contact angle, however, it significantly improved the TMC-C14 efficiency, which is a great advantage for these materials.

TMC and TMC-C14 were able to permeate through the limestone rock grains with very low-retention rates, even in brine. Both chitosan derivatives were able to significantly increase the residual oil recovery factor in the porous medium. TMC increased the oil production by about 25%. In comparison, TMC-C14 produced an oil displacement of about 16% higher, evidencing the high potential of chitosan derivatives as nontoxic chemical EOR agents for limestone reservoirs and high-salinity media.

ACKNOWLEDGMENTS

The financial support from CNPq, CAPES, and Petrobras is gratefully acknowledged. We also gratefully thank Prof. Henrique E. Toma and Dr Marcelo Nakamura from the University of São Paulo for the AFM analyses.

NOMENCLATURE

AFM	atomic force microscopy
CN	capillary number
CTAB	cetyltrimethylammonium
EOR	enhanced oil recovery
FTIR	Fourier transformed infra-red
OIP	oil initial in place
NMR	nuclear magnetic resonance
NPs	nanoparticles
PV	pore volume
TMC	trimethyl chitosan
TMC-C14	trimethyl chitosan hydrophobized with myristoyl chloride
WI	wettability inversion
wt %	weight percent
UV–Vis	ultra violet visible

REFERENCES

[1] OPEC, Annual Report, 2018 *Organization of the Petroleum Exporting Countries* **2018**, *2007* (September), 1530. https://www.opec.org/opec_web/en/publications/337.htm.
[2] J. E. Thomas, A. A. Triggia, C. A. Correia, C. V. Filho, J. A. D. Xavier, J. C. V. Machando, J. E. S. de Filho, J. L. de Paula, N. C. M. Rossi, N. E. S. Pitombo, P. C. V. M. de Gouveia, R. S. de Carvalho, R. V. Barragan, *Fundamentos de Engenharia do Petróleo* **2001**, *2*, 1271
[3] F. Li, Y. Luo, P. Hu, X. Yan, *J. Appl. Polym. Sci.* **2017**, *134*, 1.
[4] S. Al-Anssari, M. Arif, S. Wang, A. Barifcani, M. Lebedev, S. Iglauer, *Fuel* **2018**, *211*, 405.

[5] J. L. Mendoza de la Cruz, I. V. Castellanos-Ramírez, A. Ortiz-Tapia, E. Buenrostro-González, C. A. de los Durán-Valencia, S. López-Ramírez, *Colloids Surfaces A Physicochem. Eng. Asp.* **2009**, *340*, 149.

[6] B. F. Hou, Y. F. Wang, Y. Huang, *Appl. Surf. Sci.* **2015**, *330*, 56.

[7] B. Hou, R. Jia, M. Fu, Y. Huang, Y. Wang, *Energy Fuels* **2019**, *33*, 4062.

[8] R. Zhang, N. Qin, L. Peng, K. Tang, Z. Ye, *Appl. Surf. Sci.* **2012**, *258*, 7943.

[9] M. Salehi, S. J. Johnson, J. T. Liang, *Langmuir* **2008**, *24*, 14099.

[10] M. Karimi, R. S. Al-Maamari, S. Ayatollahi, N. Mehranbod, *Colloids Surfaces A Physicochem. Eng. Asp.* **2015**, *482*, 403.

[11] M. Karimi, R. S. Al-Maamari, S. Ayatollahi, N. Mehranbod, *Energy Fuels* **2016**, *30*, 819.

[12] J. V. Nicolini, H. C. Ferraz, C. P. Borges, *Fuel* **2017**, *203*, 222.

[13] D. C. Standnes, T. Austad, *J. Pet. Sci. Eng.* **2000**, *28*, 123.

[14] B. J. Abu Tarboush, M. M. Husein, *J. Colloid Interface Sci.* **2012**, *378*, 64.

[15] N. N. Nassar, *Energy Fuels* **2010**, *24*, 4116.

[16] C. Negin, S. Ali, Q. Xie, *Petroleum* **2017**, *3*, 197.

[17] H. Alhassawi, L. Romero-Zerón, *Can. J. Chem. Eng.* **2015**, *93*, 1371.

[18] D. Avila, L. Louise, G. Cavalcanti, S. Drexler, J. D. A. Rodrigues, R. S. V. Nascimento, *J. Appl. Polym. Sci.* **2016**, *43789*, 1.

[19] F. A. de Freitas, D. Keils, E. R. Lachter, C. E. B. Maia, M. I. Pais da Silva, R. S. V. Nascimento, *Fuel* **2019**, *241*, 1184.

[20] J. C. S. Rosestolato, A. Pérez-Gramatges, E. R. Lachter, R. S. V. Nascimento, *Fuel* **2019**, *239*, 403.

[21] J. C. C. Venancio, R. S. V. Nascimento, A. Pérez-Gramatges, *J. Mol. Liq.* **2020**, *308*, 113079.

[22] P. Raffa, A. A. Broekhuis, F. Picchioni, *J. Pet. Sci. Eng.* **2016**, *145*, 723.

[23] T. Yuan, Z. Liu, R. Gao, G. Hu, G. Zhang, J. Zhao, *J. Appl. Polym. Sci.* **2018**, *135*, 1.

[24] A. Domard, M. Rinaudo, C. Terrassin, *Int. J. Biol. Macromol.* **1986**, *8*, 105.

[25] G. Lopes, T. C. D. C. De Oliveira, A. Pérez-Gramatges, J. F. M. Da Silva, R. S. V. Nascimento, *J. Appl. Polym. Sci.* **2014**, *131*, 1.

[26] A. Pérez-Gramatges, C. R. V. Matheus, G. Lopes, J. C. Da Silva, R. S. V. Nascimento, *Colloids Surfaces A Physicochem. Eng. Asp.* **2013**, *418*, 124.

[27] C. Le Tien, M. Lacroix, P. Ispas-Szabo, M. A. Mateescu, *J. Controlled Release* **2003**, *93*(1), 1.

[28] C. Franco, E. Patiño, P. Benjumea, M. A. Ruiz, F. B. Cortés, *Fuel* **2013**, *105*, 408.

[29] A. Karimi, Z. Fakhroueian, A. Bahramian, N. Pour Khiabani, J. B. Darabad, R. Azin, S. Arya, *Energy Fuels* **2012**, *26*, 1028.

[30] A. M. McKenna, A. G. Marshall, R. P. Rodgers, *Energy Fuels* **2013**, *27*, 1257.

[31] M. Madhi, A. Bemani, A. Daryasafar, M. R. Khosravi Nikou, *Pet. Sci. Technol.* **2017**, *35*, 242.

[32] N. N. Nassar, A. Hassan, P. Pereira-Almao, *Energy Fuels* **2011**, *25*, 1566.

[33] E. Lichtfouse, N. Morin-Crini, M. Fourmentin, H. Zemmouri, I. O. do Carmo Nascimento, L. M. Queiroz, M. Y. M. Tadza, L. A. Picos-Corrales, H. Pei, L. D. Wilson, G. Crini, *Environ. Chem. Lett.* **2019**, *17*, 1603.

[34] V. Saruchi Kumar, *Cellulose* **2019**, *26*, 6229.

[35] P. Marcasuzaa, S. Reynaud, F. Ehrenfeld, A. Khoukh, J. Desbrieres, *Biomacromolecules* **2010**, *11*, 1684.

[36] Y. Zhang, L. Tao, S. Li, Y. Wei, *Biomacromolecules* **2011**, *12*, 2894.

[37] S. Chopra, L. Lines, D. R. Schmitt, M. Batzle, *Heavy Oils* **2010**, *1* (1), 1.

[38] M. C. Marcano, S. Kim, S. D. Taylor, U. Becker, *Chem. Geol.* **2019**, *525*, 462.

[39] B. Schuler, G. Meyer, D. Peña, O. C. Mullins, L. Gross, *J. Am. Chem. Soc.* **2015**, *137*, 9870.

[40] I. K. Yudin, G. L. Nikolaenko, E. E. Gorodetskii, V. I. Kosov, V. R. Melikyan, E. L. Markhashov, D. Frot, Y. Briolant, *J. Pet. Sci. Eng.* **1998**, *20*, 297.

[41] N. Hosseinpour, A. A. Khodadadi, A. Bahramian, Y. Mortazavi, *Langmuir* **2013**, *29*, 14135.

[42] C. Drummond, J. Israelachvili, *J. Pet. Sci. Eng.* **2004**, *45*, 61.

[43] S. Kumar, P. Panigrahi, R. K. Saw, A. Mandal, *Energy Fuels* **2016**, *30*, 2846.

[44] X. Deng, M. S. Kamal, S. Patil, S. M. S. Hussain, X. Zhou, *Energy Fuels* **2020**, *34*, 31.

[45] S. Al-Anssari, S. Wang, A. Barifcani, M. Lebedev, S. Iglauer, *Fuel* **2017**, *206*, 34.

[46] Q. Xie, F. Liu, Y. Chen, H. Yang, A. Saeedi, M. M. Hossain, *J. Pet. Sci. Eng.* **2019**, *174*, 418.

[47] I. K. Shaik, J. Song, S. L. Biswal, G. J. Hirasaki, P. K. Bikkina, & C. P. Aichele, Effect of brine type and ionic strength on the wettability alteration of naphthenic-acid-adsorbed calcite surfaces. *Journal of Petroleum Science and Engineering* **2019**, *185*, 106567.

[48] K. Kumar, E. Dao, K. K. Mohanty, *J. Colloid Interface Sci.* **2005**, *289*, 206.

[49] L. N. Nwidee, M. Lebedev, A. Barifcani, M. Sarmadivaleh, S. Iglauer, *J. Colloid Interface Sci.* **2017**, *504*, 334.

[50] C. Jiang, W. Zeng, F. Liu, B. Tang, Q. J. Liu, *Phys. Chem. Solids* **2019**, *131*, 1.

[51] Y. Bouhadda, T. Fergoug, E. Y. Sheu, D. Bendedouch, A. Krallafa, D. Bormann, A. Boubguira, *Fuel* **2008**, *87*, 3481.

[52] R. M. Balabin, R. Z. Syunyaev, T. Schmid, J. Stadler, E. I. Lomakina, R. Zenobi, *Energy Fuels* **2011**, *25*, 189.

[53] W. A. Abdallah, Y. Yang, *Energy Fuels* **2012**, *26*, 6888.

[54] Druetta P., Picchioni F., Polymer and nanoparticles flooding as a new method for Enhanced Oil Recovery *Journal of Petroleum Science and Engineering* **2019**, *177*, 479. http://dx.doi.org/10.1016/j.petrol.2019.02.070.

[55] Gutierrez, M. E., Gaona, S. J., Calvete, F. E., Botett, J. A. & Ferrari, J. V., Paper presented at In SPE International Conference on Oilfield Chemistry, Society of Petroleum Engineers. 8-9 April, Galveston, Texas, USA, **2019**, March.

[56] K. Ma, L. Cui, Y. Dong, T. Wang, C. Da, G. J. Hirasaki, S. L. Biswal, *J. Colloid Interface Sci.* **2013**, *408*, 164.

[57] R. Saha, R. V. S. Uppaluri, P. Tiwari, *Colloids Surfaces A* **2017**, *531*, 121.

[58] S. Iglauer, Y. Wu, P. Shuler, Y. Tang, W. A. G. Iii, *J. Pet. Sci. Eng.* **2010**, *71*, 23.

[59] Telmadarreie, A.; Trivedi, J. J. Soc. Pet. Eng.-SPE Int. Heavy Oil Conf. Exhib. 2018, HOCE 2018 **2018**.

[60] S. Drexler, F. P. Souza, E. L. Correia, T. M. G. Silveira, P. Couto, *Brazilian J. Pet. Gas* **2019**, *12*, 195.

[61] Drexler, S.; Hoerlle, F. O.; Silveira, T. M. G.; Cavadas, L. A.; Couto, P. Offshore Technology. Conf. Brasil 2019, OTCB 2019 **2020**.
[62] E. Nourafkan, Z. Hu, D. Wen, *J. Colloid Interface Sci.* **2018**, *519*, 44.
[63] N. Nguyen, C. Dang, S. E. Gorucu, L. Nghiem, Z. Chen, *Fuel* **2019**, *263*, 116542.
[64] S. C. Ayirala, S. M. Al-Enezi, A. A. Al-Yousef, *J. Pet. Sci. Eng.* **2017**, *157*, 530.

How to cite this article: dos Santos Francisco AD, Grasseschi D, Nascimento RSV. Wettability alteration of oil-wet carbonate rocks by chitosan derivatives for application in enhanced oil recovery. *J Appl Polym Sci*. 2021;138:e50098. https://doi.org/10.1002/app.50098